

Exploring pion emission properties of (strange) hidden-charm molecular pentaquarks in a chiral quark model

Li-Cheng Sheng^{1,3}, Yu-Jie Tang¹, Yu-Xin Wan¹, Rui Chen^{1,2*},[†] and Dian-Yong Chen^{3‡}

¹Key Laboratory of Low-Dimensional Quantum Structures and Quantum Control of Ministry of Education, Department of Physics and Synergetic Innovation Center for Quantum Effects and Applications, Hunan Normal University, Changsha 410081, China

²Hunan Research Center of the Basic Discipline for Quantum Effects and Quantum Technologies, Hunan Normal University, Changsha 410081, China

³ School of Physics, Southeast University, Nanjing 210094, People's Republic of China
(Dated: November 19, 2025)

The internal structure of the exotic P_c and P_{cs} pentaquarks remains an open question. To address this, we demonstrate that pion emission serves as a sensitive probe by calculating its properties within a molecular scenario using the chiral quark model and coupled-channel effects. Our results reveal a strong dependence of the decay widths on the internal structure and spatial wave functions. We therefore expect this study to stimulate experimental measurements of these decays, which are crucial for determining the nature of these states and guiding the search for further molecular partners.

I. INTRODUCTION

Over the past twenty years, experiments have observed numerous exotic hadronic structures that are distinct from conventional mesons (composed of a quark-antiquark pair) and baryons (composed of three quarks). Studying these states cannot only help to establish and refine the hadron spectrum but also provide a powerful approach for deepening our understanding of complex non-perturbative phenomena in quantum chromodynamics (QCD).

A prime example of these exotic structures is the family of hidden-charm pentaquarks. In 2015, the LHCb Collaboration reported the first observations of two hidden-charm structures, labeled as $P_c(4380)$ and $P_c(4450)$, in $\Lambda_b^0 \rightarrow J/\psi p K^-$ decay process [1]. Theoretically, the discovery of $P_c(4380)$ and $P_c(4450)$ stimulated vigorous discussions concerning their internal structure and underlying production mechanisms. Various interpretations were proposed, including molecular hadronic states, compact pentaquarks, and non-resonant explanations[2–7]. Given that the masses of $P_c(4380)$ and $P_c(4450)$ lie close to the thresholds of charmed baryon and anti-charmed meson pairs, the molecular state hypothesis emerged as a popular explanation. In fact, theorists had predicted the existence of such hidden-charm molecular pentaquarks prior to their experimental observation[8–12]. Detailed reviews of the theoretical progress on these initial P_c states can be found in Refs. [13–15]. This theoretical landscape, however, was reshaped by subsequent experimental data.

With the accumulation of more data, the LHCb Collaboration performed a new analysis of the same decay channel in 2019. This analysis not only revealed a new

narrow structure, $P_c(4312)$, but also resolved the previously observed $P_c(4450)$ into two distinct substructures, labeled as $P_c(4440)$ and $P_c(4457)$ [16]. The discovery of these fine structures provided stronger support for interpreting hidden-charm pentaquarks as meson-baryon molecular states. Although the molecular picture gained significant traction following the 2019 results, it is not the only viable interpretation. Several studies continue to argue that these P_c states are compact pentaquarks [17–22].

Beyond the fundamental question of molecular versus compact structure, a further debate exists regarding the specific quantum numbers of these states within the molecular framework. For example, in our previous work [23], we investigated the interactions between a charmed baryon and an anti-charmed meson using the one-boson-exchange (OBE) model, including coupled-channel effects. We found that $P_c(4312)$ can be identified as the $\Sigma_c \bar{D}$ molecule with $I(J^P) = 1/2(1/2^-)$, while $P_c(4440)$ and $P_c(4457)$ can be identified as the $\Sigma_c \bar{D}^*$ molecules with $1/2(1/2^-)$ and $1/2(3/2^-)$, respectively. In Ref. [24], the authors proposed that $P_c(4312)$ can be well interpreted as the $\Sigma_c^{*+} D^-$ bound state with $J^P = 1/2^-$, while $P_c(4440)$ and $P_c(4457)$ could be interpreted as the $\Sigma_c^+ \bar{D}^0$ bound state with $1/2^-$, the $\Sigma_c^{*++} D^-$ and $\Sigma_c^+ \bar{D}^{*0}$ bound states with $3/2^-$, or the $\Sigma_c^{*+} \bar{D}^{*0}$ bound state with $5/2^-$, based on their previous QCD sum rule studies.

This pattern of discovery followed by theoretical ambiguity was repeated with the observation of a strange hidden-charm pentaquark. In 2020, the LHCb Collaboration reported evidence for the strange hidden-charm pentaquark $P_{cs}(4459)$ in $\Xi_b^- \rightarrow J/\psi \Lambda K^-$ with a statistical significance of 3.1σ [25]. Theoretically, various explanations for $P_{cs}(4459)$ have been proposed, including molecular states, compact pentaquarks, and triangle singularity mechanisms [26–36]. Because $P_{cs}(4459)$ lies just below the $\Xi_c \bar{D}^*$ threshold, the molecular scenario has attracted considerable attention. Nevertheless, there is ongoing discussion about the internal

*Corresponding author

[†]Electronic address: chenrui@hunnu.edu.cn

[‡]Electronic address: chendy@seu.edu.cn

structure of $P_{cs}(4459)$ as a hadronic molecule [28, 37–40]. For instance, since the spin-parity of $P_{cs}(4459)$ has not been determined experimentally, a key theoretical question is whether it can be assigned as a $\Xi_c \bar{D}^{(*)}$ molecule with $I(J^P) = 0(1/2^-)$ or $0(3/2^-)$ [39, 41–43]. In Ref. [44], we performed a coupled-channel analysis of $\Xi_c \bar{D}^*/\Xi_c^* \bar{D}/\Xi_c' \bar{D}^*/\Xi_c^* \bar{D}^*$ using the OBE model. We found that $P_{cs}(4459)$ can be described as a bound state in this coupled-channel system with $I(J^P) = 0(3/2^-)$, where the dominant components are $\Xi_c \bar{D}^*$ and $\Xi_c^* \bar{D}$. Beside the $\Xi_c \bar{D}^*$ molecular explanation, A. Feijoo et al. proposed that $P_{cs}(4459)$ is associated to the state coupled mostly to $\Xi_c' \bar{D}$ [45], after studied the interaction in coupled channels of pseudoscalar mesons and vector mesons with baryons of $J^P = 1/2^+$ and $3/2^+$.

The cumulative evidence from the P_c and P_{cs} states thus presents a clear challenge: while abundant theoretical models exist, a definitive method to pinpoint their internal structure is lacking. Therefore, a more comprehensive and systematic investigation is required. As is well known, decay properties are highly sensitive to the wave functions of the interacting particles. Consequently, we propose that exploring pion π emission properties provides a crucial and sensitive probe. Since π emission involves spin-related interactions, our results can help identify molecular configurations, especially their spin-parity quantum numbers. In the meson-baryon molecular scenario, the π emission occurs at the constituent hadrons, as illustrated in Figure 1. In Ref. [46], the authors investigated similar processes, namely the pionic transition from $Y(4260)$ to $Z_c(3900)$.

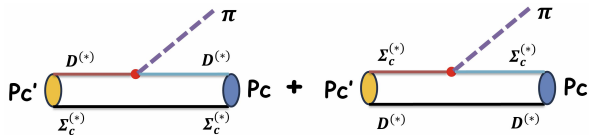


FIG. 1: The π emission process between the P_c molecular states.

To this end, in this work we adopt the chiral quark model to derive the decay amplitudes for the π emission processes between possible P_c/P_{cs} molecules. In addition to focusing on the reported P_c/P_{cs} states as molecules, we also calculate the π emission decay widths for transitions between the reported states and other possible (strange) hidden-charm molecular pentaquarks predicted in our previous works [23, 44]. Through these efforts, we aim to provide new methods for searching for possible hidden-charm molecular partners.

This paper is organized as follow. After introduction, the detailed deduction of the π emission interactions between possible P_c/P_{cs} states molecules systems is given in Sec. II. In Sec. III, we present the numerical results. The paper ends with a summary in Sec. IV.

II. FRAMEWORK

In this work, we adopt the chiral quark model to deduce the π emission interactions. The corresponding effective Lagrangians can be constructed as follows [47–54]:

$$\mathcal{L} = \frac{\delta}{\sqrt{2}f_p} \bar{\psi}_j \gamma_\mu \gamma_5 \psi_j \vec{I} \cdot \vec{\partial}^\mu \phi_p. \quad (1)$$

Here, I is an isospin operator. δ and f_p denote the coupling strength for the quark-pseudoscalar-meson interaction and the pseudoscalar meson decay constant, respectively. ϕ_p and ψ_j represent the pseudoscalar meson field and the j th light quark field, respectively. In a Pauli-Dirac representation, the quark field can be approximated as

$$\psi_j \simeq \left(\frac{\sigma_j \cdot \mathbf{P}_i}{E_i + M_i} + \frac{\sigma_j \cdot \mathbf{P}_j}{2m_j} \right), \quad (2)$$

where \mathbf{P}_i is the momentum of the initial molecular state. The quantities \mathbf{P}_j , σ_j , and m_j are the internal momentum, spin operator, and mass of the j th quark within the molecular state, respectively.

Through a non-relativistic reduction, the non-relativistic form of \mathcal{L} up to order $1/m$ can be obtained:

$$\mathcal{L} = g \sum_j (\mathcal{G} \sigma_j \cdot \mathbf{q} + h \sigma_j \cdot \mathbf{p}_j) F(\mathbf{q}^2) I_j \varphi_m. \quad (3)$$

In the Eq.(3), σ_j and \mathbf{p}_j are the spin operator and momentum operator of the j th light quark in the molecular state. $\varphi_m = e^{-i\mathbf{q} \cdot \mathbf{r}_j}$ is the plane wave function of the emitted light meson. The constants are defined as $g = i\delta \sqrt{(E_i + M_i)(E_f + M_f)} / (\sqrt{2}f_M)$, $\mathcal{G} = -\left(\frac{\omega_m}{E_f + M_f} + 1\right)$, and $h = \omega_m / 2\mu_q$, where (E_i, M_i) and (E_f, M_f) are the energy and mass of the initial and final molecular states, respectively. ω_m and \mathbf{q} are the energy and three momentum of the emitted meson, respectively. The reduced mass μ_q is expressed as $\mu_q = m_j m_{j'} / (m_j + m_{j'})$, where m_j and $m_{j'}$ are the mass of j -th quark in the initial and final molecular states. Following Ref. [49, 53], the isospin operator I_j is given by

$$I_j = \begin{cases} a_j^\dagger(u) a_j(d) & \text{for } \pi^-, \\ a_j^\dagger(d) a_j(u) & \text{for } \pi^+, \\ \frac{1}{\sqrt{2}} [a_j^\dagger(u) a_j(u) - a_j^\dagger(d) a_j(d)] & \text{for } \pi^0, \end{cases} \quad (4)$$

where $a_j^\dagger(u, d)$ and $a_j(u, d)$ are the creation and annihilation operators for u and d quarks. To suppress unphysical high-momentum contributions, a form factor $F(\mathbf{q}^2)$ is introduced, expressed as $F(\mathbf{q}^2) = \sqrt{\Lambda^2 / (\Lambda^2 + \mathbf{q}^2)}$.

The model parameters used in this work are listed in Table I. As in Refs. [49, 53], the quark-meson coupling strength is set to $\delta = 0.557$. The cut-off parameter Λ is taken as $\Lambda = 0.66$ GeV, following the discussions in Refs. [51, 54–57].

TABLE I: The parameters adopted in this work.

$m_u(\text{GeV})$	$m_d(\text{GeV})$	$m_s(\text{GeV})$	$m_c(\text{GeV})$	δ	$\Lambda(\text{GeV})$	$f_\pi(\text{GeV})$
0.45	0.45	0.55	1.68	0.557	0.66	0.093

For the π meson emission between possible $P_{c(s)}$ molecules, the strong decay amplitude is given by

$$\mathcal{M}[\mathcal{B} \rightarrow \mathcal{B}' + \pi] = \langle \mathcal{B}' | \mathcal{H}^{NR} | \mathcal{B} \rangle, \quad (5)$$

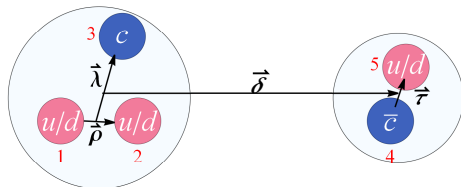
where \mathcal{B} and \mathcal{B}' are the initial and final molecular states. The corresponding partial decay width is calculated as

$$\Gamma = \frac{1}{8\pi} \frac{|q|}{M_i^2} \frac{1}{2J_i + 1} \sum_{J_{f_z}} |\mathcal{M}_{J_{i_z} J_{f_z}}|^2. \quad (6)$$

Here, J_i is the total angular momentum quantum number of the initial molecular state, and J_{i_z} and J_{f_z} are the third components of the total momenta of the initial and final molecular states, respectively.

In Fig. 2, Jacobi coordinates $\mathbf{R} = \boldsymbol{\rho}, \boldsymbol{\lambda}, \boldsymbol{\tau}, \boldsymbol{\delta}$ are used to describe the spatial wave function of the hadronic molecular states. The total spatial wave function for the initial and final states is then expressed as a product: $\phi(\boldsymbol{\rho})\phi(\boldsymbol{\lambda})\phi(\boldsymbol{\tau})\phi(\boldsymbol{\delta})$. These Jacobi coordinates are related to the quark coordinates \mathbf{r}_j by

$$\begin{aligned} \boldsymbol{\rho} &= \mathbf{r}_2 - \mathbf{r}_1, \\ \boldsymbol{\lambda} &= \mathbf{r}_3 - \frac{m_1 \mathbf{r}_1 + m_2 \mathbf{r}_2}{m_1 + m_2}, \\ \boldsymbol{\tau} &= \mathbf{r}_5 - \mathbf{r}_4, \\ \boldsymbol{\delta} &= \frac{m_4 \mathbf{r}_4 + m_5 \mathbf{r}_5}{m_4 + m_5} - \frac{m_1 \mathbf{r}_1 + m_2 \mathbf{r}_2 + m_3 \mathbf{r}_3}{m_1 + m_2 + m_3}. \end{aligned} \quad (7)$$

FIG. 2: The Jacobi coordinates of the $\Sigma_c \bar{D}^{(*)}$ molecular states.

The spatial wave function between the constituent hadrons, $\phi(\boldsymbol{\delta})$, is obtained by solving the Schrödinger equation. We employ the simple harmonic oscillator (SHO) wave function to describe the internal spatial wave functions of the mesons and baryons [58–62]:

$$\phi_{n,l,m}(\beta, \mathbf{r}) = \sqrt{\frac{2n!}{\Gamma(n+l+\frac{3}{2})}} L_n^{l+\frac{1}{2}}(\beta^2 r^2) \beta^{l+\frac{3}{2}} e^{-\frac{\beta^2 r^2}{2}} r^l Y_{lm}(\Omega). \quad (8)$$

Here, $L_n^{l+\frac{1}{2}}$ is the associated Laguerre polynomial and Y_{lm} is the spherical harmonic function. Refs. [63–65] explored light meson decays using SHO wave functions with

β in the range of 3.5–4.0 GeV. In this work, we adopt $\beta = 4.0$ GeV.

The involved flavor wave functions $|I, I_3\rangle$ are

$$\left| \frac{1}{2}, \frac{1}{2} \right\rangle = \sqrt{\frac{2}{3}} |\Sigma_c^{(*)++} D^{(*)-}\rangle - \frac{1}{\sqrt{3}} |\Sigma_c^{(*)+} \bar{D}^{(*)0}\rangle, \quad (9)$$

$$\left| \frac{1}{2}, -\frac{1}{2} \right\rangle = \frac{1}{\sqrt{3}} |\Sigma_c^{(*)+} D^{(*)-}\rangle - \sqrt{\frac{2}{3}} |\Sigma_c^{(*)0} \bar{D}^{(*)0}\rangle, \quad (10)$$

$$|0, 0\rangle = \frac{1}{\sqrt{2}} |\Xi_c^{(*)+} D^{(*)-}\rangle - \frac{1}{\sqrt{2}} |\Xi_c^{(*)0} \bar{D}^{(*)0}\rangle, \quad (11)$$

$$|1, 1\rangle = |\Xi_c^{(*)+} \bar{D}^{(*)0}\rangle, \quad (12)$$

$$|1, 0\rangle = \frac{1}{\sqrt{2}} |\Xi_c^{(*)+} D^{(*)-}\rangle + \frac{1}{\sqrt{2}} |\Xi_c^{(*)0} \bar{D}^{(*)0}\rangle, \quad (13)$$

$$|1, -1\rangle = |\Xi_c^{(*)0} D^{(*)-}\rangle. \quad (14)$$

Furthermore, the spin wave functions $|S, S_z\rangle$ of these molecular states are constructed as:

$$|S, S_z\rangle = \sum_{S_z^B, S_z^M} C_{S_z^B, S_z^M}^{S, S_z} |S^B, S_z^B\rangle |S^M, S_z^M\rangle. \quad (15)$$

Here, the superscript B and the superscript M denote the spins of the baryon and meson constituents, respectively. The subscript z indicates the third component of the spin. The total spin and its third component for the molecular state are S and S_z , respectively.

III. NUMERICAL RESULTS

Before producing our calculations, we would like to provide a brief introduction to the (strange) hidden-charm molecular pentaquarks discussed in this work. In Refs. [23, 44], we used one-boson-exchange (OBE) effective potentials to study the mass spectrum of such states, composed of a charmed baryon and an anti-charmed meson. Our analysis successfully reproduced the masses of the $P_c(4312)$, $P_c(4440)$, $P_c(4457)$, and $P_{cs}(4459)$ within the meson-baryon molecular picture but also suggested that the $P_c(4380)$ observed in 2015 [1] can be identified as a coupled-channel molecule of $\Sigma_c^* \bar{D} / \Sigma_c \bar{D}^* / \Sigma_c^* \bar{D}^*$. In this interpretation, the probability for the $\Sigma_c^* \bar{D}$ channel exceeds 87%. Furthermore, we predicted a series of other possible (strange) hidden-charm molecular pentaquarks. The mass positions of these states are shown in Figure 3. For convenience, we label them as follows:

$$\begin{aligned} P_{c0}^{\Sigma_c^* \bar{D}^*} &\sim \Sigma_c^* \bar{D}^* [1/2(1/2^-)], & P_{cs0}^{\Xi_c^* \bar{D}^*} &\sim \Xi_c^* \bar{D}^* [0(1/2^-)], \\ P_{c1}^{\Sigma_c^* \bar{D}^*} &\sim \Sigma_c^* \bar{D}^* [1/2(3/2^-)], & P_{cs1}^{\Xi_c^* \bar{D}^*} &\sim \Xi_c^* \bar{D}^* [0(3/2^-)], \\ P_{c2}^{\Sigma_c^* \bar{D}^*} &\sim \Sigma_c^* \bar{D}^* [1/2(5/2^-)], & P_{cs2}^{\Xi_c^* \bar{D}^*} &\sim \Xi_c^* \bar{D}^* [0(5/2^-)], \\ P_c(4312) &\sim \Sigma_c \bar{D} / \Sigma_c \bar{D}^* / \Sigma_c^* \bar{D}^* [1/2(1/2^-)], \\ P_c(4380) &\sim \Sigma_c^* \bar{D} / \Sigma_c \bar{D}^* / \Sigma_c^* \bar{D}^* [1/2(3/2^-)], \\ P_c(4440) &\sim \Sigma_c \bar{D}^* / \Sigma_c^* \bar{D}^* [1/2(1/2^-)], \\ P_c(4457) &\sim \Sigma_c \bar{D}^* / \Sigma_c^* \bar{D}^* [1/2(3/2^-)], \end{aligned}$$

smaller than those for the $J^P = 3/2^-$ assignment of the $P_c(4457)$.

In summary, we find the following order of magnitude for the pion emission widths in the $P_c(4457) \rightarrow P_c(4312) + \pi$ process:

$$\Gamma(1/2^-) : \Gamma(3/2^-) : \Gamma^C(3/2^-) = 0.10 : 3.00 : 9.00, \quad (17)$$

where $\Gamma(1/2^-)$ and $\Gamma(3/2^-)$ denote the decay widths with $P_c(4457)$ as the pure $\Sigma_c \bar{D}^*$ molecule with $I(J^P) = 1/2(1/2^-)$ and $1/2(3/2^-)$, respectively, and $\Gamma^C(3/2^-)$ represents the decay width with both $P_c(4457)$ and $P_c(4312)$ treated as coupled-channel molecules [23]. These results provide important and helpful insights for understanding the internal structures and quantum number assignments of the $P_c(4457)$ and $P_c(4312)$ states.

B. $P_c^{\Sigma_c^* \bar{D}^*} \rightarrow P_c(4312) + \pi$

We next compute the decay widths for $\Sigma_c^* \bar{D}^*$ molecules with $I(J^P) = 1/2(1/2^-, 3/2^-, 5/2^-)$ decaying into $P_c(4312) + \pi$. For initial states with $I(J^P) = 1/2(1/2^-, 3/2^-)$, the decay proceeds via P -wave interactions. In a single-channel analysis where $P_c(4312)$ is treated as a pure $\Sigma_c \bar{D}$ molecule with $1/2(1/2^-)$, these pion emission processes are forbidden due to the absence of common configurations between the initial and final molecular states.

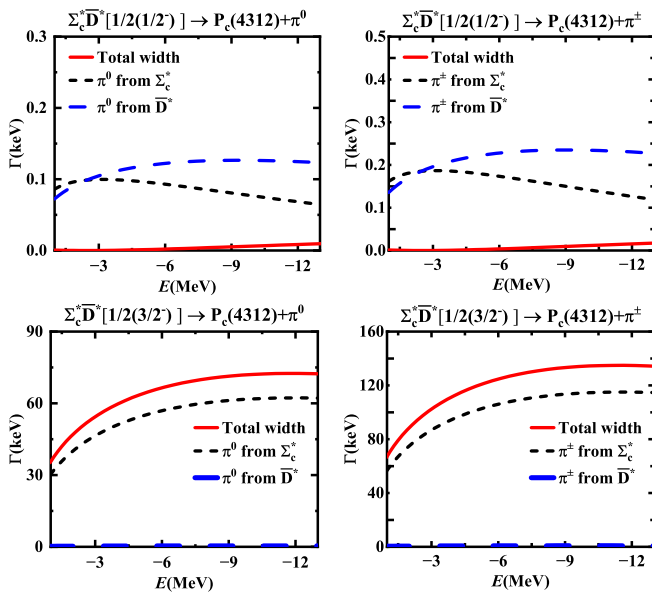


FIG. 4: The pion emission widths for $\Sigma_c^* \bar{D}^*$ molecules with $I(J^P) = 1/2(1/2^-, 3/2^-)$ decaying into $P_c(4312)$.

When coupled-channel effects are included, as illustrated in Figure 4, the situation changes. Our results show that for the decay $P_c^{\Sigma_c^* \bar{D}^*} [1/2(1/2^-)] \rightarrow P_c(4312) + \pi^{\pm,0}$, the partial widths are less than 0.1 keV for binding energies E ranging from 0 to -12 MeV. These small

widths are dominated by pion emission from the anti-charmed meson components, $\bar{D}^{(*)} \rightarrow \bar{D}^{(*)} + \pi$. The contribution from pion emission off the charmed baryon components is negligible. In line with the isospin factor relations, the decay width for neutral pion emission is approximately a factor of two smaller than for charged pion emission.

For the decay $P_c^{\Sigma_c^* \bar{D}^*} [1/2(3/2^-)] \rightarrow P_c(4312) + \pi^{\pm}$, the partial width ranges from 60 to 140 keV for initial state binding energies $E > -15$ MeV. In this case, pion emission from the charmed baryon components plays a dominant role. Consistent with the isospin relation $\mathcal{M}(P_c^i \rightarrow P_c^f + \pi^{\pm}) = \sqrt{2} \mathcal{M}(P_c^i \rightarrow P_c^f + \pi^0)$, the neutral pion emission width is again a factor of two smaller than its charged counterpart.

Finally, for the decay $P_c^{\Sigma_c^* \bar{D}^*} [1/2(5/2^-)] \rightarrow P_c(4312) + \pi$, the process must proceed via an F -wave interaction. This higher partial wave is expected to be strongly suppressed compared to the P -wave decays discussed above.

C. $P_c^{\Sigma_c^* \bar{D}^*} \rightarrow P_c(4380) + \pi$

For the decay processes $P_c^{\Sigma_c^* \bar{D}^*} \rightarrow P_c(4380) + \pi$, the available phase space is relatively limited compared to the decays to $P_c(4312) + \pi$. This significantly influences the resulting decay widths, as shown in Figure 5. The limited phase space manifests in two key aspects: first, the decay widths for neutral and charged pion emission become comparable, despite the isospin relation $\mathcal{M}(P_c^i \rightarrow P_c^f + \pi^{\pm}) = \sqrt{2} \mathcal{M}(P_c^i \rightarrow P_c^f + \pi^0)$; second, the decay widths decrease with increasing binding energy of the $\Sigma_c^* \bar{D}^*$ molecules.

We first discuss the decay properties assuming $P_c(4380)$ as a pure $\Sigma_c^* \bar{D}$ molecule with $1/2(3/2^-)$. In this scenario, pion emission occurs via the transition between the anti-charmed meson components, $\bar{D}^* \rightarrow \bar{D} + \pi$. Since the charmed baryon components act as spectators, the decay width is independent of the total spin of the initial $\Sigma_c^* \bar{D}^*$ state. Our calculations show decay widths on the order of several keV for initial states with $J^P = 1/2^-, 3/2^-$, and $5/2^-$.

In the coupled channel case, where $P_c(4380)$ is a mixture of $\Sigma_c^* \bar{D}$, $\Sigma_c \bar{D}^*$, and $\Sigma_c^* \bar{D}^*$ with $1/2(3/2^-)$, pion emission from the charmed baryon components also contributes to the total decay width. Consequently, the decay widths for initial $\Sigma_c^* \bar{D}^*$ states with different spin-parities differ substantially. Figure 5 shows the dependence of these decay widths on the binding energy.

For the process $P_c^{\Sigma_c^* \bar{D}^*} [1/2(1/2^-)] \rightarrow P_c(4380) + \pi$, the pion emission amplitude from the charmed baryon component is stronger than that from the anti-charmed meson component. However, these two amplitudes interfere destructively, resulting in a very small total decay width of less than 0.5 keV.

In contrast, for the process $P_c^{\Sigma_c^* \bar{D}^*} [1/2(3/2^-)] \rightarrow P_c(4380) + \pi$, the individual amplitudes from the meson

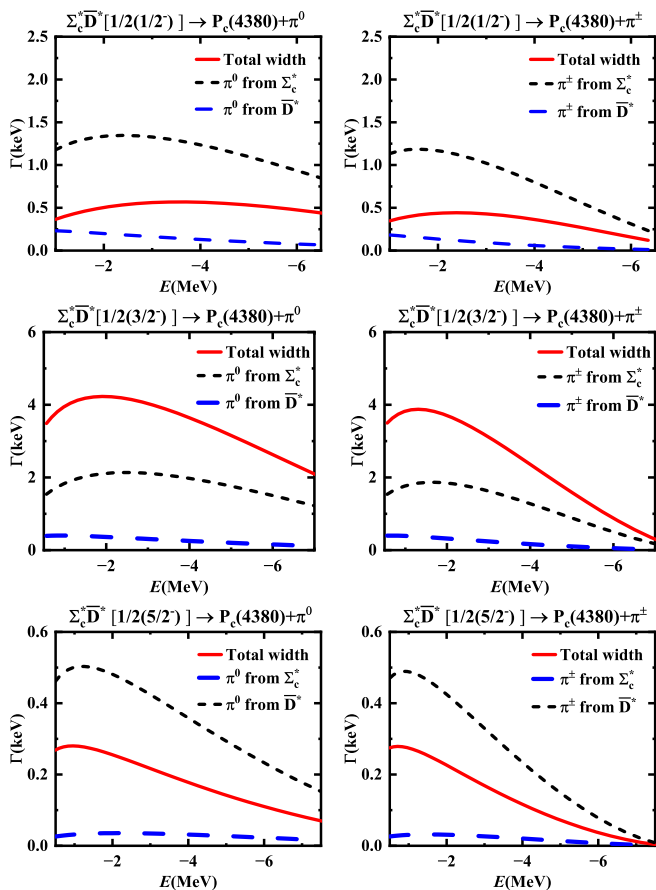


FIG. 5: The pion emission widths for the $\Sigma_c^* \bar{D}^*$ molecules with $I(J^P) = 1/2(1/2^-, 3/2^-, 5/2^-)$ decaying into $P_c(4380)$.

and baryon components are of similar magnitude but interfere constructively. This leads to a significantly larger decay width, as shown in Figure 5, where both charged and neutral pion emission widths can reach a few keV for binding energies $E > -10$ MeV.

For the process $P_c^{\Sigma_c^* \bar{D}^*} [1/2(5/2^-)] \rightarrow P_c(4380) + \pi$, the total decay width is less than 1 keV. This is dominated by the $\bar{D}^* \rightarrow \bar{D}^{(*)} + \pi$ interactions, the pion emission from the charmed baryon component is very small. Furthermore, these two contributions interfere destructively.

D. $P_{cs}^i \rightarrow P_{cs}^f + \pi$

We next compute the pion emission widths for transitions between possible strange hidden-charm molecular pentaquarks, $P_{cs}^i \rightarrow P_{cs}^f + \pi$, within the coupled-channel framework. The processes discussed, constrained by quantum number conservation, are:

- $P_{cs}^{\Xi_c^* \bar{D}^*} [1(3/2^-)] \rightarrow P_{cs}(4338) + \pi$,
- $P_{cs}^{\Xi_c^* \bar{D}^*} [1(3/2^-)] \rightarrow P_{cs}^{\Xi_c^* \bar{D}^*} [0, 1(1/2^-)] + \pi$,
- $P_{cs}^{\Xi_c^* \bar{D}^*} [0(1/2^-, 3/2^-)] \rightarrow P_{cs}^{\Xi_c^* \bar{D}^*} [1(1/2^-)] + \pi$,

- $P_{cs}^{\Xi_c^* \bar{D}^*} [0(1/2^-, 3/2^-)] \rightarrow P_{cs}^{\Xi_c^* \bar{D}^*} [1(1/2^-)] + \pi$,
- $P_{cs}^{\Xi_c^* \bar{D}^*} [0(1/2^-, 3/2^-, 5/2^-)] \rightarrow P_{cs}^{\Xi_c^* \bar{D}^*} [1(3/2^-)] + \pi$.

TABLE II: The π emission widths between possible strange hidden-charm molecular pentaquarks. Here, the units of the widths are keV.

Processes	π^0	π^\pm
$P_{cs1}^{\Xi_c^* \bar{D}^*} [1(3/2^-)] \rightarrow P_{cs}(4338) + \pi$	130 ~ 280	100 ~ 250
$P_{cs1}^{\Xi_c^* \bar{D}^*} [1(3/2^-)] \rightarrow P_{cs0}^{\Xi_c^* \bar{D}^*} [0(1/2^-)] + \pi$	4.0	0.6
$P_{cs1}^{\Xi_c^* \bar{D}^*} [1(3/2^-)] \rightarrow P_{cs1}^{\Xi_c^* \bar{D}^*} [1(1/2^-)] + \pi$	25 ~ 50	3 ~ 8
$P_{cs0}^{\Xi_c^* \bar{D}^*} [0(1/2^-)] \rightarrow P_{cs1}^{\Xi_c^* \bar{D}^*} [1(1/2^-)] + \pi$	1.5	0.2
$P_{cs1}^{\Xi_c^* \bar{D}^*} [0(3/2^-)] \rightarrow P_{cs1}^{\Xi_c^* \bar{D}^*} [1(1/2^-)] + \pi$	0.8	0.1
$P_{cs0}^{\Xi_c^* \bar{D}^*} [0(1/2^-)] \rightarrow P_{cs1}^{\Xi_c^* \bar{D}^*} [1(1/2^-)] + \pi$	30 ~ 100	20 ~ 90
$P_{cs1}^{\Xi_c^* \bar{D}^*} [0(3/2^-)] \rightarrow P_{cs1}^{\Xi_c^* \bar{D}^*} [1(1/2^-)] + \pi$	50 ~ 150	30 ~ 150
$P_{cs0}^{\Xi_c^* \bar{D}^*} [0(1/2^-)] \rightarrow P_{cs1}^{\Xi_c^* \bar{D}^*} [1(3/2^-)] + \pi$	0.5	0.1
$P_{cs1}^{\Xi_c^* \bar{D}^*} [0(3/2^-)] \rightarrow P_{cs1}^{\Xi_c^* \bar{D}^*} [1(3/2^-)] + \pi$	1.7	0.3
$P_{cs2}^{\Xi_c^* \bar{D}^*} [0(5/2^-)] \rightarrow P_{cs1}^{\Xi_c^* \bar{D}^*} [1(3/2^-)] + \pi$	2.8	0.4

The corresponding decay widths are summarized in Table II. In these calculations, the binding energies for both the initial and final molecular states were varied within the range $E > -10$ MeV, while the binding energy of $P_{cs}(4338)$ was fixed at $E = -1.06$ MeV. Our findings are as follows:

1. For the process $P_{cs1}^{\Xi_c^* \bar{D}^*} [1(3/2^-)] \rightarrow P_{cs}(4338) + \pi$, the partial widths for neutral and charged pion emission are very similar. This occurs despite the isospin relation for the decay amplitude, $\mathcal{M}(P_{cs}^i \rightarrow P_{cs}^f + \pi^\pm) = -\mathcal{M}(P_{cs}^i \rightarrow P_{cs}^f + \pi^0)$, due to nearly identical phase space for both final states. When the initial molecular state has a binding energy $E > -10$ MeV, the decay widths range from 130 to 280 keV for π^0 and from 100 to 250 keV for π^\pm . These decays proceed exclusively via pion emission from the charmed baryon components, $\Xi_c^{(*)} \rightarrow \Xi_c^{(*)} + \pi$.
2. For the process $P_{cs1}^{\Xi_c^* \bar{D}^*} [1(3/2^-)] \rightarrow P_{cs0}^{\Xi_c^* \bar{D}^*} [0(1/2^-)] + \pi$, the partial widths are only a few keV, being strongly suppressed by the limited phase space. The dominant contributions are attributed to interactions involving the charmed baryons, $\Xi_c^{(*)} \rightarrow \Xi_c^{(*)} + \pi$.
3. For the process $P_{cs1}^{\Xi_c^* \bar{D}^*} [1(3/2^-)] \rightarrow P_{cs1}^{\Xi_c^* \bar{D}^*} [1(1/2^-)] + \pi$, the partial widths can reach several tens of keV, significantly larger than the previous case. This enhancement results from constructive interference among the amplitudes from different coupled channels. Pion emission from the charmed baryon components remains the dominant mechanism.

4. For the following processes, the partial widths are very small, typically only a few keV:

- $P_{cs0}^{\Xi_c^{\pm}\bar{D}^*} [0(1/2^-)] \rightarrow P_{cs1}^{\Xi_c^{\pm}\bar{D}} [1(1/2^-)] + \pi$,
- $P_{cs1}^{\Xi_c^{\pm}\bar{D}^*} [0(3/2^-)] \rightarrow P_{cs1}^{\Xi_c^{\pm}\bar{D}} [1(1/2^-)] + \pi$,
- $P_{cs0}^{\Xi_c^{\pm}\bar{D}^*} [0(1/2^-)] \rightarrow P_{cs1}^{\Xi_c^{\pm}\bar{D}} [1(1/2^-)] + \pi$,
- $P_{cs1}^{\Xi_c^{\pm}\bar{D}^*} [0(3/2^-)] \rightarrow P_{cs1}^{\Xi_c^{\pm}\bar{D}} [1(3/2^-)] + \pi$,
- $P_{cs2}^{\Xi_c^{\pm}\bar{D}^*} [0(5/2^-)] \rightarrow P_{cs1}^{\Xi_c^{\pm}\bar{D}} [1(3/2^-)] + \pi$.

The decay widths are primarily due to pion emission between the anti-charmed meson components, $\bar{D}^{(*)} \rightarrow \bar{D}^{(*)} + \pi$. The extremely limited phase space leads to significant differences between the neutral and charged pion emission widths, even though the isospin relation $\mathcal{M}(P_{cs}^i \rightarrow P_{cs}^f + \pi^\pm) = -\mathcal{M}(P_{cs}^i \rightarrow P_{cs}^f + \pi^0)$ holds.

5. For the processes $P_{cs0}^{\Xi_c^{\pm}\bar{D}^*} [0(1/2^-)] \rightarrow P_{cs1}^{\Xi_c^{\pm}\bar{D}} [1(1/2^-)] + \pi$ and $P_{cs1}^{\Xi_c^{\pm}\bar{D}^*} [0(3/2^-)] \rightarrow P_{cs1}^{\Xi_c^{\pm}\bar{D}} [1(1/2^-)] + \pi$ processes, pion emission from the charmed baryon components plays a significant role. The partial widths are around several tens to one hundred keV for $E > -10$ MeV, and the widths for neutral and charged pion emission are again comparable.

IV. SUMMARY

The discovery of hidden-charm pentaquarks constitutes a milestone in hadron physics, not only by confirming a new form of matter but, more importantly, by opening a new frontier for probing the strong interaction in the non-perturbative regime. Despite extensive theoretical and experimental progress over the past decade, fundamental questions regarding their internal structure and quantum numbers remain actively debated.

In this context, the study of light meson emission decays emerges as a powerful and independent diagnostic tool. These radiative processes are highly sensitive to the strong interactions at play and are intimately linked to the spatial wave functions and quantum numbers of the involved hadrons, thereby providing crucial information to discriminate between different structural models.

In this work, we have investigated the pion emission properties of P_c/P_{cs} states within a molecular scenario, focusing on both experimentally observed states [1, 16, 25, 66] and our own theoretical predictions [23, 44].

Our framework is based on the chiral quark model, incorporating coupled-channel effects to derive the pion emission interactions. The numerical calculations utilize the spatial wave functions obtained from our previous dynamical studies [23, 44].

In Figure 6, we present the pion emission widths between possible P_c/P_{cs} molecules. Our key findings are as follows:

- The calculated pion emission widths exhibit a strong dependence on the quantum number configurations and the available phase space.
- Coupled-channel effects play an essential role in determining the decay amplitudes.
- In most processes, the partial decay width for neutral pion emission is greater than that for charged pion emission.
- We identify several decay channels with sizable widths, such as $P_{c1}^{\Sigma_c^{\pm}\bar{D}^*} [1/2(3/2^-)] \rightarrow P_c(4312) + \pi$, $P_{cs1}^{\Xi_c^{\pm}\bar{D}} [1(3/2^-)] \rightarrow P_{cs}(4338) + \pi$, $P_{cs0}^{\Xi_c^{\pm}\bar{D}^*} [0(1/2^-)] \rightarrow P_{cs1}^{\Xi_c^{\pm}\bar{D}} [1(1/2^-)] + \pi$ and $P_{cs1}^{\Xi_c^{\pm}\bar{D}^*} [0(3/2^-)] \rightarrow P_{cs1}^{\Xi_c^{\pm}\bar{D}} [1(1/2^-)] + \pi$, which represent promising signatures for future experimental detection.

In summary, the systematic patterns we have identified in pion emission decays provide a new set of criteria for testing molecular interpretations and assigning quantum numbers to the observed (strange) hidden-charm pentaquarks. We strongly encourage experimental collaborations to test these predictions. Furthermore, this methodological approach can be extended to guide the search for other, yet-unobserved (strange) hidden-charm molecular pentaquarks, particularly those composed of excited constituents.

ACKNOWLEDGMENTS

We would like to thank Hui-Hua Zhong and Xian-Hui Zhong for valuable discussions. This project is supported by the National Natural Science Foundation of China under Grants Nos. 12305139, 12175037, 12335001, and in part by National Key Research and Development Program under the contract No. 2024YFA1610503. Rui Chen is also supported by the Xiaoxiang Scholars Program of Hunan Normal University.

[1] R. Aaij et al. [LHCb], Observation of $J/\psi p$ Resonances Consistent with Pentaquark States in $\Lambda_b^0 \rightarrow J/\psi K^- p$ Decays, *Phys. Rev. Lett.* **115**, 072001 (2015).
 [2] R. Chen, X. Liu, X. Q. Li and S. L. Zhu, Identifying exotic hidden-charm pentaquarks, *Phys. Rev. Lett.* **115**,

no.13, 132002 (2015).
 [3] H. X. Chen, W. Chen, X. Liu, T. G. Steele and S. L. Zhu, Towards exotic hidden-charm pentaquarks in QCD, *Phys. Rev. Lett.* **115**, no.17, 172001 (2015).
 [4] M. Karliner and J. L. Rosner, New Exotic Meson

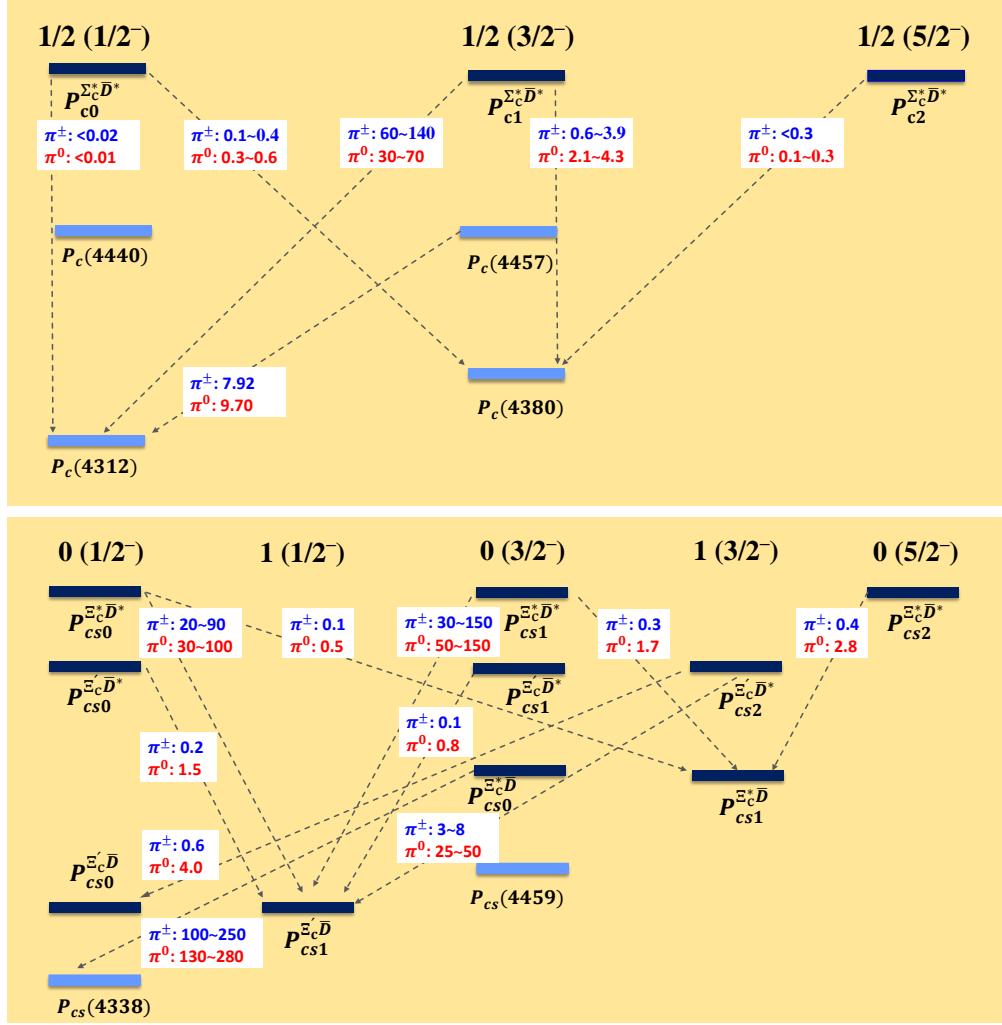


FIG. 6: A summary of the pion emission properties of possible P_c/P_{cs} molecules. Here, the decay widths are in the unit of keV.

- and Baryon Resonances from Doubly-Heavy Hadronic Molecules, *Phys. Rev. Lett.* **115**, no.12, 122001 (2015).
- [5] L. Maiani, A. D. Polosa and V. Riquer, The New Pentaquarks in the Di-quark Model, *Phys. Lett. B* **749**, 289-291 (2015).
- [6] R. F. Lebed, The Pentaquark Candidates in the Dynamical Di-quark Picture, *Phys. Lett. B* **749**, 454-457 (2015).
- [7] Z. G. Wang and T. Huang, Analysis of the $\frac{1}{2}^\pm$ pentaquark states in the diquark model with QCD sum rules, *Eur. Phys. J. C* **76**, no.1, 43 (2016).
- [8] J. J. Wu, R. Molina, E. Oset and B. S. Zou, Prediction of narrow N^* and Λ^* resonances with hidden charm above 4 GeV, *Phys. Rev. Lett.* **105**, 232001 (2010).
- [9] Z. C. Yang, Z. F. Sun, J. He, X. Liu and S. L. Zhu, The possible hidden-charm molecular baryons composed of anti-charmed meson and charmed baryon, *Chin. Phys. C* **36**, 6-13 (2012).
- [10] W. L. Wang, F. Huang, Z. Y. Zhang and B. S. Zou, $\Sigma_c \bar{D}$ and $\Lambda_c \bar{D}$ states in a chiral quark model, *Phys. Rev. C* **84**, 015203 (2011).
- [11] J. J. Wu, T. S. H. Lee and B. S. Zou, Nucleon Resonances with Hidden Charm in Coupled-Channel Models, *Phys. Rev. C* **85**, 044002 (2012).
- [12] X. Q. Li and X. Liu, A possible global group structure for exotic states, *Eur. Phys. J. C* **74**, no.12, 3198 (2014).
- [13] H. X. Chen, W. Chen, X. Liu and S. L. Zhu, The hidden-charm pentaquark and tetraquark states, *Phys. Rept.* **639**, 1-121 (2016).
- [14] Y. Dong, A. Faessler and V. E. Lyubovitskij, Description of heavy exotic resonances as molecular states using phenomenological Lagrangians, *Prog. Part. Nucl. Phys.* **94**, 282-310 (2017).
- [15] F. K. Guo, C. Hanhart, U. G. Meißner, Q. Wang, Q. Zhao and B. S. Zou, Hadronic molecules, *Rev. Mod. Phys.* **90**, no.1, 015004 (2018) [erratum: *Rev. Mod. Phys.* **94**, no.2, 029901 (2022)].
- [16] R. Aaij et al. [LHCb], Observation of a narrow pentaquark state, $P_c(4312)^+$, and of two-peak structure of the $P_c(4450)^+$, *Phys. Rev. Lett.* **122**, no.22, 222001 (2019).
- [17] A. Ali and A. Y. Parkhomenko, Interpretation of the narrow $J/\psi p$ Peaks in $\Lambda_b \rightarrow J/\psi p K^-$ decay in the compact diquark model, *Phys. Lett. B* **793**, 365-371 (2019).
- [18] H. Mutuk, Neural Network Study of Hidden-Charm Pentaquark Resonances, *Chin. Phys. C* **43**, no.9, 093103

- (2019).
- [19] Z. G. Wang, Analysis of the $P_c(4312)$, $P_c(4440)$, $P_c(4457)$ and related hidden-charm pentaquark states with QCD sum rules, *Int. J. Mod. Phys. A* **35**, no.01, 2050003 (2020).
- [20] J. B. Cheng and Y. R. Liu, $P_c(4457)^+$, $P_c(4440)^+$, and $P_c(4312)^+$: molecules or compact pentaquarks? *Phys. Rev. D* **100**, no.5, 054002 (2019).
- [21] X. Z. Weng, X. L. Chen, W. Z. Deng and S. L. Zhu, Hidden-charm pentaquarks and P_c states, *Phys. Rev. D* **100**, no.1, 016014 (2019).
- [22] A. Pimikov, H. J. Lee and P. Zhang, Hidden charm pentaquarks with color-octet substructure in QCD Sum Rules, *Phys. Rev. D* **101**, no.1, 014002 (2020).
- [23] R. Chen, Z. F. Sun, X. Liu and S. L. Zhu, Strong LHCb evidence supporting the existence of the hidden-charm molecular pentaquarks, *Phys. Rev. D* **100**, no.1, 011502 (2019).
- [24] H. X. Chen, W. Chen and S. L. Zhu, Possible interpretations of the $P_c(4312)$, $P_c(4440)$, and $P_c(4457)$, *Phys. Rev. D* **100**, no.5, 051501 (2019).
- [25] R. Aaij et al. [LHCb], Evidence of a $J/\psi\Lambda$ structure and observation of excited Ξ^- states in the $\Xi_b^- \rightarrow J/\psi\Lambda K^-$ decay, *Sci. Bull.* **66**, 1278-1287 (2021).
- [26] B. S. Zou, Building up the spectrum of pentaquark states as hadronic molecules, *Sci. Bull.* **66**, 1258 (2021).
- [27] M. Karliner and J. L. Rosner, Strange pentaquarks and excited Ξ hyperons in $\Xi_b^- \rightarrow J/\psi\Lambda K^-$ final states, *Sci. Bull.* **66**, no.13, 1256 (2021).
- [28] F. Z. Peng, M. J. Yan, M. Sánchez Sánchez and M. P. Valderrama, The $P_{cs}(4459)$ pentaquark from a combined effective field theory and phenomenological perspective, *Eur. Phys. J. C* **81**, no.7, 666 (2021).
- [29] J. T. Zhu, L. Q. Song and J. He, $P_{cs}(4459)$ and other possible molecular states from $\Xi_c^{(*)}\bar{D}^{(*)}$ and $\Xi_c'\bar{D}^{(*)}$ interactions, *Phys. Rev. D* **103**, no.7, 074007 (2021).
- [30] X. Hu and J. Ping, Investigation of hidden-charm pentaquarks with strangeness $S = -1$, *Eur. Phys. J. C* **82**, no.2, 118 (2022).
- [31] C. W. Xiao, J. J. Wu and B. S. Zou, Molecular nature of $P_{cs}(4459)$ and its heavy quark spin partners, *Phys. Rev. D* **103**, no.5, 054016 (2021).
- [32] C. R. Deng, Compact hidden charm pentaquark states and QCD isomers, *Phys. Rev. D* **105**, no.11, 116021 (2022).
- [33] Z. G. Wang, Analysis of the $P_{cs}(4459)$ as the hidden-charm pentaquark state with QCD sum rules, *Int. J. Mod. Phys. A* **36**, no.10, 2150071 (2021).
- [34] J. Ferretti and E. Santopinto, The new $P_{cs}(4459)$, $Z_{cs}(3985)$, $Z_{cs}(4000)$ and $Z_{cs}(4220)$ and the possible emergence of flavor pentaquark octets and tetraquark nonets, *Sci. Bull.* **67**, 1209 (2022).
- [35] K. Azizi, Y. Sarac and H. Sundu, Investigation of $P_{cs}(4459)^0$ pentaquark via its strong decay to $\Lambda J/\psi$, *Phys. Rev. D* **103**, no.9, 094033 (2021).
- [36] C. W. Shen, H. J. Jing, F. K. Guo and J. J. Wu, Exploring Possible Triangle Singularities in the $\Xi_b^- \rightarrow K^- J/\psi\Lambda$ Decay, *Symmetry* **12**, no.10, 1611 (2020).
- [37] M. W. Li, Z. W. Liu, Z. F. Sun and R. Chen, Magnetic moments and transition magnetic moments of Pc and Pcs states, *Phys. Rev. D* **104**, no.5, 054016 (2021).
- [38] Q. Wu, D. Y. Chen and R. Ji, Production of $P_{cs}(4459)$ from Ξ_b Decay, *Chin. Phys. Lett.* **38**, no.7, 071301 (2021).
- [39] J. X. Lu, M. Z. Liu, R. X. Shi and L. S. Geng, Understanding $P_{cs}(4459)$ as a hadronic molecule in the $\Xi_b^- \rightarrow J/\psi\Lambda K^-$ decay, *Phys. Rev. D* **104**, no.3, 034022 (2021).
- [40] F. Yang, Y. Huang and H. Q. Zhu, Strong decays of the $P_{cs}(4459)$ as a $\Xi_c\bar{D}^*$ molecule, *Sci. China Phys. Mech. Astron.* **64**, no.12, 121011 (2021).
- [41] M. L. Du, Z. H. Guo and J. A. Oller, Insights into the nature of the $P_{cs}(4459)$, *Phys. Rev. D* **104**, no.11, 114034 (2021).
- [42] U. Özdem, Magnetic dipole moments of the hidden-charm pentaquark states: $P_c(4440)$, $P_c(4457)$ and $P_{cs}(4459)$, *Eur. Phys. J. C* **81**, no.4, 277 (2021).
- [43] F. Gao and H. S. Li, Magnetic moments of hidden-charm strange pentaquark states*, *Chin. Phys. C* **46**, no.12, 123111 (2022).
- [44] R. Chen and X. Liu, Mass behavior of hidden-charm open-strange pentaquarks inspired by the established P_c molecular states, *Phys. Rev. D* **105**, no.1, 014029 (2022).
- [45] A. Feijoo, W. F. Wang, C. W. Xiao, J. J. Wu, E. Oset, J. Nieves and B. S. Zou, A new look at the Pcs states from a molecular perspective, *Phys. Lett. B* **839**, 137760 (2023).
- [46] D. Y. Chen, Y. B. Dong, M. T. Li and W. L. Wang, Pionic transition from $Y(4260)$ to $Z_c(3900)$ in a hadronic molecular scenario, *Eur. Phys. J. A* **52**, no.10, 310 (2016).
- [47] A. Manohar and H. Georgi, Chiral Quarks and the Non-relativistic Quark Model, *Nucl. Phys. B* **234**, 189-212 (1984).
- [48] K. L. Wang, Y. X. Yao, X. H. Zhong and Q. Zhao, Strong and radiative decays of the low-lying S - and P -wave singly heavy baryons, *Phys. Rev. D* **96**, no.11, 116016 (2017).
- [49] X. h. Zhong and Q. Zhao, Strong decays of heavy-light mesons in a chiral quark model, *Phys. Rev. D* **78**, 014029 (2008).
- [50] L. Y. Xiao, K. L. Wang, Q. f. Lu, X. H. Zhong and S. L. Zhu, Strong and radiative decays of the doubly charmed baryons, *Phys. Rev. D* **96**, no.9, 094005 (2017).
- [51] R. H. Ni, J. J. Wu and X. H. Zhong, Unified unquenched quark model for heavy-light mesons with chiral dynamics, *Phys. Rev. D* **109**, no.11, 116006 (2024).
- [52] Y. H. Zhou, W. J. Wang, L. Y. Xiao and X. H. Zhong, Strong decays of the low-lying $1P$ - and $1D$ -wave Σ_c baryons, *Phys. Rev. D* **108**, no.1, 014019 (2023).
- [53] X. H. Zhong and Q. Zhao, Charmed baryon strong decays in a chiral quark model, *Phys. Rev. D* **77**, 074008 (2008).
- [54] H. H. Zhong, M. S. Liu, R. H. Ni, M. Y. Chen, X. H. Zhong and Q. Zhao, Unified study of nucleon and Δ baryon spectra and their strong decays with chiral dynamics, *Phys. Rev. D* **110**, no.11, 116034 (2024).
- [55] Y. W. Yu, Z. Y. Zhang, P. N. Shen and L. R. Dai, Quark quark potential from chiral symmetry, *Phys. Rev. C* **52**, 3393-3398 (1995).
- [56] J. Vijande, F. Fernandez and A. Valcarce, Constituent quark model study of the meson spectra, *J. Phys. G* **31**, 481 (2005).
- [57] A. Valcarce, H. Garcilazo and J. Vijande, Towards an understanding of heavy baryon spectroscopy, *Eur. Phys. J. A* **37**, 217-225 (2008).
- [58] D. M. Li and S. Zhou, On the nature of the $\pi(2)(1880)$, *Phys. Rev. D* **79**, 014014 (2009).
- [59] J. F. Liu and G. J. Ding, Bottomonium Spectrum with Coupled-Channel Effects, *Eur. Phys. J. C* **72**, 1981 (2012).

- [60] B. J. Lai, F. L. Wang and X. Liu, Investigating the M1 radiative decay behaviors and the magnetic moments of the predicted triple-charm molecular-type pentaquarks, *Phys. Rev. D* **109**, no.5, 054036 (2024).
- [61] C. K. Zhang, F. L. Wang, S. Q. Luo and X. Liu, Electromagnetic properties of possible triple-charm molecular hexaquarks, *Eur. Phys. J. C* **85**, no.5, 582 (2025).
- [62] F. L. Wang, S. Q. Luo, H. Y. Zhou, Z. W. Liu and X. Liu, Exploring the electromagnetic properties of the $\Xi_c^{(\prime,*)}\bar{D}_s^*$ and $\Omega_c^{(*)}\bar{D}_s^*$ molecular states, *Phys. Rev. D* **108**, no.3, 034006 (2023).
- [63] T. Barnes, N. Black and P. R. Page, Strong decays of strange quarkonia, *Phys. Rev. D* **68**, 054014 (2003).
- [64] E. S. Ackleh, T. Barnes and E. S. Swanson, On the mechanism of open flavor strong decays, *Phys. Rev. D* **54**, 6811-6829 (1996).
- [65] T. Barnes, F. E. Close, P. R. Page and E. S. Swanson, Higher quarkonia, *Phys. Rev. D* **55**, 4157-4188 (1997).
- [66] R. Aaij et al. [LHCb], Observation of a $J/\psi\Lambda$ Resonance Consistent with a Strange Pentaquark Candidate in $B^- \rightarrow J/\psi\Lambda\bar{p}$ Decays, *Phys. Rev. Lett.* **131**, no.3, 031901 (2023).
- [67] F. L. Wang and X. Liu, Emergence of molecular-type characteristic spectrum of hidden-charm pentaquark with strangeness embodied in the $P_{\psi_s}^\Lambda(4338)$ and $P_{cs}(4459)$, *Phys. Lett. B* **835**, 137583 (2022).
- [68] U. Özdem, Investigation of magnetic moment of $P_{cs}(4338)$ and $P_{cs}(4459)$ pentaquark states, *Phys. Lett. B* **836**, 137635 (2023).
- [69] M. J. Yan, F. Z. Peng, M. Sánchez Sánchez and M. Pavon Valderrama, $P_{\psi_s}^\Lambda(4338)$ pentaquark and its partners in the molecular picture, *Phys. Rev. D* **107**, no.7, 7 (2023).
- [70] X. Z. Ling, J. X. Lu, M. Z. Liu and L. S. Geng, $P_c(4457) \rightarrow P_c(4312)\pi/\gamma$ in the molecular picture, *Phys. Rev. D* **104**, no.7, 074022 (2021).
- [71] G. J. Wang, L. Y. Xiao, R. Chen, X. H. Liu, X. Liu and S. L. Zhu, Probing hidden-charm decay properties of P_c states in a molecular scenario, *Phys. Rev. D* **102**, no.3, 036012 (2020).
- [72] J. E. Bartelt et al. [CLEO], Observation of the radiative decay $D^{*+} \rightarrow D^+\gamma$, *Phys. Rev. Lett.* **80**, 3919-3923 (1998).
- [73] J. P. Lees et al. [BaBar], Measurement of the $D^*(2010)^+$ meson width and the $D^*(2010)^+ - D^0$ mass difference, *Phys. Rev. Lett.* **111**, no.11, 111801 (2013).